Strength Characteristics of Weathered Granite

By

Koichi AKAI*, Toshihisa ADACHI**, Kazuo YAMAMOTO***
and Yuzo OHNISHI*

(Received June 30, 1976)

Abstract

Weathered granite, which widely distributed in Japan, was tested by a triaxial testing apparatus to investigate its mechanical properties in the consolidated-undrained condition.

This rock, classified as a soft rock, causes much trouble in the construction of civil engineering structures. However, its mechanical behavior has not been studied enough to understand the strength characteristics. In this paper, it was found that the general behavior of the weathered granite was very similar to that of clay. The comparison between these materials has been discussed. The strength parameters were obtained from yield points which were defined by two different methods. The physical meanings of these yield points were also discussed.

1. Introduction

Recently, with the construction of large scale structures like dams, bridges, underground power-houses, *etc.*, it has been recognized that the safety of such structures are strongly dependent on the stability of the foundation rock. For centuries building on rock has been synonymous with building safely. During the past few decasdes this situation has changed, and now with increases on the load intensity of structure and the difficulty of site selections due to various social restrictions, the demands for rock mechanics are highly raised to investigate and understand the engineering properties of rock and rock masses. The rock and rock masses are roughly categorized into two parts; soft rock and hard rock. Although it is very important to study the properties of both kinds of rock, the comprehensive study on soft rock has not been sufficiently done. Especially in Japan, soft rocks such as weathered granite, green tuff, mud stone, *etc.* are widely spread and caused much trouble in the construction of civil engineering structures. In

* Department of Transportation Engineering
** Disaster Prevention Research Institute
*** Osaka Prefectural Technical College

this study, we discuss the strength characteristics of soft rock in relation to soil, since we had a chance to investigate the mechanical behavior of weathered granite.

2. Experimental Apparatus and Test Procedure

One of triaxial loading apparatus used in this study is shown in Fig. 1. The pressure to confine a specimen is applied up to 30 kg/cm^2, depending on the strength of the soft rock. The size of the specimen is 50 mm in diameter and 100 mm in height. An axial load is applied at the constant displacement rate in the range of 0.0002–0.2 mm/min. As shown in Fig. 2, water in the specimen is drained through a paper which enclosed the specimen and through a porous disc at the bottom pedestal to a bullet, by which the amount of drained water is measured. Measurement of pore pressure induced in the specimen is done by a small pressure transducer beneath the disc. Rock specimens are cut to suit the dimensions of the test apparatus from rock blocks which are carefully excavated from in-situ rock mass at a tunnel site. The sample is enclosed by a thin rubber tube and is subjected to a predetermined confining pressure and back pressure.

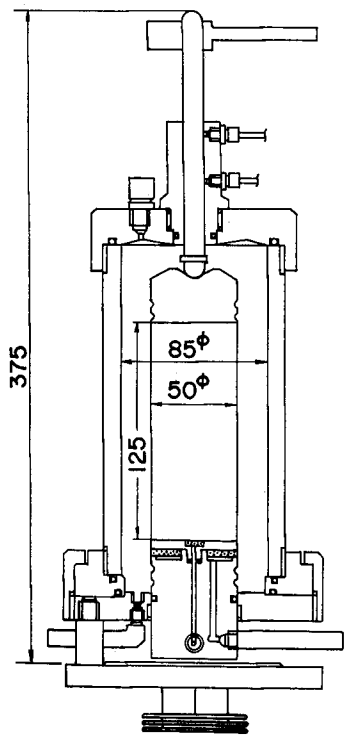

Fig. 1. A triaxial cell and loading apparatus.

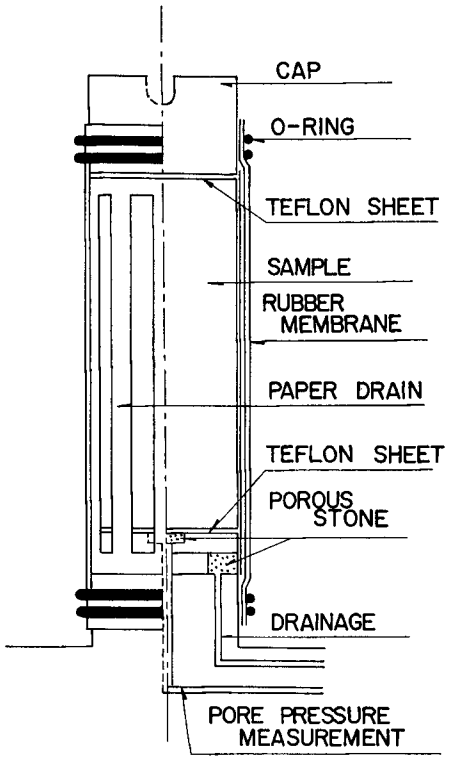

Fig. 2. Detailed specimen set-up in a triaxial cell.

3. Stress-Strain Relationship

The research on the stress-strain characteristics of soil and rock materials has been carried out by several people. However, study on weathered granite with more than 10% of porosity has not been done at all, due to the difficulty of making undisturbed test samples. We overcame these difficulties and obtained valuable results on the mechanical properties of weathered granite.

In general, the stress-strain relationship of geologic materials is highly affected by the confining pressure, strain rate and stress histories, *etc.*. By preliminary study, we had found that the stress-strain relation of weathered granite was mostly expressed in the way as shown in Fig. 3 (a) or (b). In these figures, the vertical axis is the deviator stress $(\sigma_1-\sigma_3)$, the pore pressure (u) and the abscissa is the axial strain (ε_1). The stress-strain curve in Fig. 3 (a) has an initial Young's modulus E_i and approaches asymptotically a maximum strength $(\sigma_1-\sigma_3)_f=1/b$ in a hyperbolic form which was originally published by Kondner[1]. In his paper, he explained that the stress-strain relation of consolidated undrained clay could be expressed by a hyperbola, such as an equation

$$\sigma_1-\sigma_3 = \varepsilon_1/(a+b\varepsilon_1) \qquad (1)$$

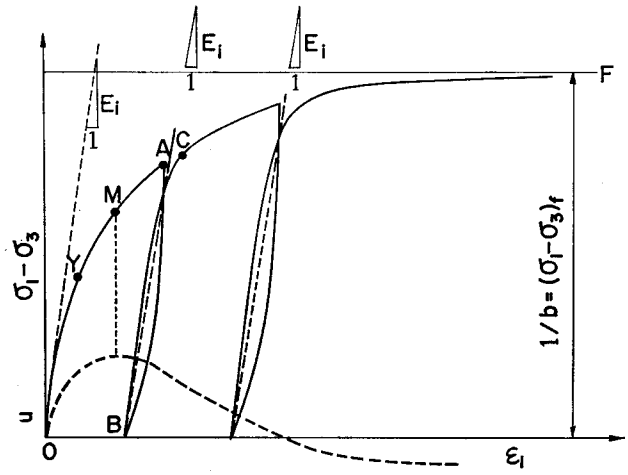

Fig. 3 (a). Diagramatic representation of stress-strain behavior of strain-hardening type rock.

where $a=1/E_i$, $b=1/(\sigma_1-\sigma_3)_f$. These parameters are determined by laboratory experiments depending upon the strain rate, confining pressure, over-consolidation ratio, conditions of confining, *etc.*. In order to obtain the parameters a and b from experimental data, Eq. (1) is reformed as follows;

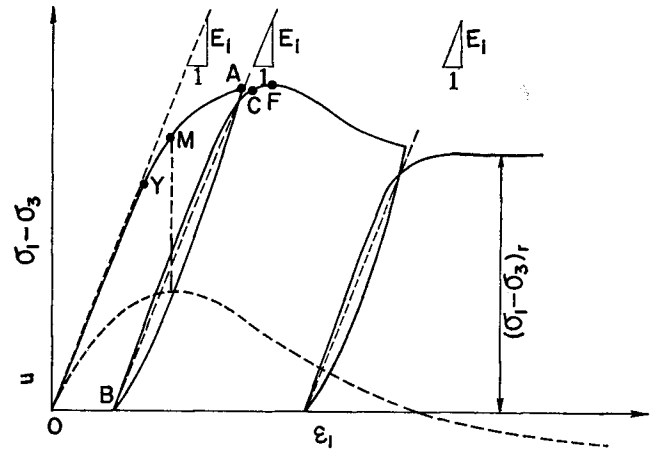

Fig. 3 (b). Diagramatic representation of stress-strain behavior of strain-softening type rock.

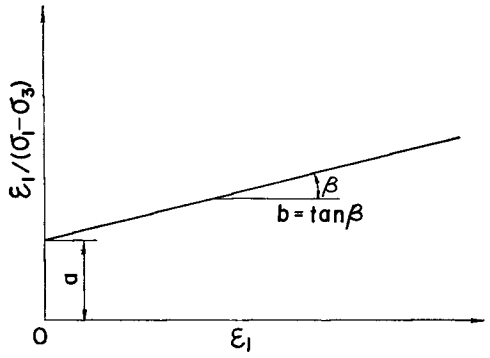

Fig. 4. Transformed linear hyperbolic plot of Kondner's hyperbola.

$$\varepsilon_1/(\sigma_1-\sigma_3) = a+b\varepsilon_1 \qquad (2)$$

The left hand side of the equation is linear to the axial strain and Eq. (2) can be plotted in the form of Fig. 4, where a is an intersection of the vertical axis and b is a slope angle of the straight line.

When the increased axial load was unloaded from point A in Figs. 3 (a) and (b) at which the stress level is beyond a yield point of the material, there exists a permanent deformation OB at a stress $(\sigma_1-\sigma_3)=0$. If the specimen is loaded again, it shows a hysteresis up to point C from which the curve coincides with the original stress-strain relation and approaches the maximum strength. From the feature of this curve, it is known that the sample shows the elastic-plastic behavior

and the slope of the unloading-reloading curve is almost the same as the initial Young's modulus E_i. Duncan and Chang[2] tested sand and found that the E_t is dependent upon the confining pressure, and is expressed by the following equation;

$$E_i = K_i \cdot P_a(\sigma_3/P_a)^n \qquad (3)$$

where K_i and n are non-dimensional material parameters and P_a is an atmospheric pressure. The stress-strain curve shown in Fig. 3 (a) is called a strain-hardening type, in which the stress increases monotonically with the strain increase. However, it is well known that rock materials in general, over-consolidated clay, dense sand and sedimentary soft rock show a peak stress, and afterwards drop down to a residual stress with the strain increase as shown in Fig. 3 (b). Since this residual strength is related to a long-term stability of the rock mass such as progressive failure, its value should not be overlooked from the laboratory data.

The other feature to be emphasized in Figs. 3 (a) and (b) is the behavior of the induced pore pressure u. In an undrained triaxial test, the pore pressure increases with the axial stress and shows a peak point, after which it tends to decrease when the deformation continues. This means that, in a drained triaxial test, the volume of the rock specimen starts to expand at this point (point M in the figures). This feature of the material is called dilatancy, and point M can be considered to be a certain special point for the geologic material, a drastic change of the structure in the material.

So far, we have discussed the strain-hardening elasto-plastic and dilatant behavior of the geologic material. However, in order to analyze the material response to the external load, it is preferable to determine the limit of the elastic deformation, *i.e.* yield stress point. The turning point of the volume change curve described above is in a state of material yielding. The other way of de-

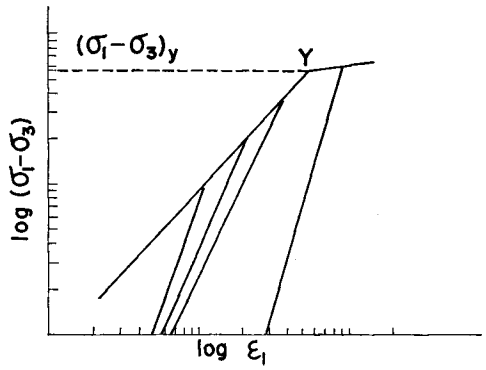

Fig. 5. Diagramatic representation of stress-strain curve plotted in log-log scale.

termining a yield point is done by plotting the stress-strain curve in a log-log scale diagram as shown in Fig. 5. The breaking point of the straight line in the figure is also in a state of yield, since unloading at less than this stress level causes a very little permanent deformation and also a noticeable irreversible deformation occurs beyond point Y. This stress point seems to be related to the long-term strength of the material under a sustained load. We discuss this feature later in this paper, in comparison with experimental evidence.

4. Laboratory Measurements and Results

Two different types of weathered granite have been selected to investigate the mechanical properties. The range from *A* class (very hard, fresh rock) to *D* class (very soft, weak rock) is used in the usual rock classification. The weathered granite is mostly calssified as class *C* or class *D*, depending upon the degree of weathering and alteration. One kind of weathered granite tested in our laboratory (we call them sample I) is in class D_L. Each class is subdivided into *H*(high), *M* (midium) and *L* (low). Class D_L is weakest in that class. The other sample (sample II) is in class C_M-C_L.

(A) Sample I

This sample is heavily weathered and its mineral ingredients are altered to clay. Cracks and discontinuities are not found in the specimen, which was sampled by using a specially designed core cutter like a thin-walled cylinder. The specimen was easily trimmed by a wire saw to suit the dimensions of the experimental apparatus.

Table 1 shows the physical properties of sample I, in which we can see that the material is very porous and clayey (porosity about 40%).

(i) Stress-Strain-Pore Pressure

The triaxial shearing test was carried out in a consolidated-undrained condi-

Table 1. Physical properties of rock sample I. w: water content, e: void ratio, γ : density of soil, γ_d: dry density, G_s: specific gravity of solid, S_r: degree of saturation

Sample	w	e	γ	γ_d	G_s	S_r
	%	—	g/cm³	g/cm³	—	%
Site 1	17.2	0.50	1.968	1.682		
Site 2	22.6	.650	1.921	1.571		
Site 3	17.0	0.49	1.962	1.676	2.60	90.0
Site 4	16.3	0.47	1.953	1.680		
Average	18.2	0.53	1.948	1.651		

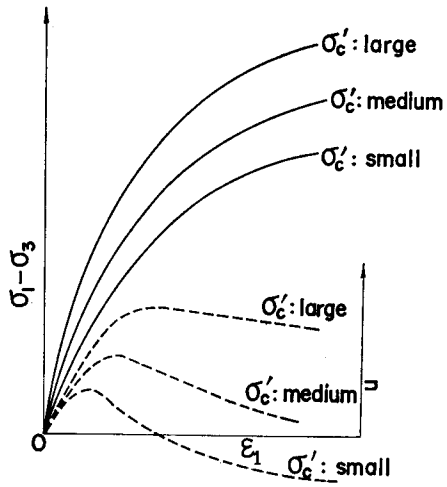

Fig. 6. Behavior of stress-strain-pore pressure of strain-hardening type rock subjected to different confining pressures.

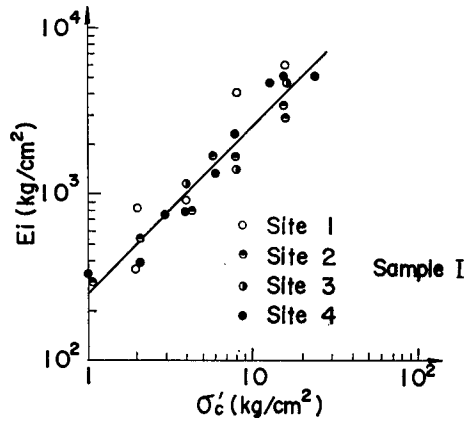

Fig. 7. Variations of initial Young's modulus E_i depending upon the consolidation pressure: Sample I.

tion with a constant confining pressure and a constant strain rate of about 0.04% /min. The experimental results show the relations between stress (deviator stress)-strain (axial strain) and induced pore pressure as shown in Fig. 6. The stress-strain curves rapidly rise at the initial part due to the seating errors, and gradually bend even at a low stress level. At the high stress level these stresses still increase with the strain. This can be interpreted that the elsatic and plastic strains are induced in the specimen at a low stress level and the plastic strain is dominant at a high stress level. However, since the unloading and reloading cycles of the triaxial test were not performed, we are not very certain about its interpretation.

Determination of initial Young's modulus E_i by approximating the data to Kondner's hyperbola shows that E_i increases with the increase of the consolidation pressure σ_c' as shown in Fig. 7, and their relation E_i and σ_c' is expressed in the following equation;

$$E_i = 2.5 \times 10^2 \sigma_c' \qquad (4)$$

Under a low confining pressure, the pore pressure induced by the axial stress increases gradually until it shows a peak value, at 1–2% of small shear strain, whose magnitude is about 30–50% of the axial stress. After the peak, it rapidly decreases to a negative value (relative to the initial back pressure). On the other hand, under a high confining pressure, the pore pressure stays in the positive range even after attaining a peak value of 50–90% of the axial stress at a strain of 3–5.4%. The positive and negative signs of the pore pressure indicate the tendency of the material characteristics of dilatancy, which is the contraction and expansion

of the specimen volume. Therefore, the above observation and discussion disclose that the behavior of the specimens under a consolidation pressure 1–2 kg/cm^2 resembles that of the over-consolidated clay and the behavior of the normally consolidated clay if the specimens are subjected to a confining pressure of over 3 kg/cm^2.

(ii) Strength Parameters

While several methods have been known to determine the strength of the intact rock, the distinct way of strength determination of a soft rock, which shows a non-linear stress-strain relation over the all stress ranges, is not established yet. Therefore, we now estimate the strength of soft rock by the following two methods which were briefly discussed in the previous section. The first method is that if a stress-strain curve is plotted in the log-log scale, it is approximated by two lines broken at the yield point. However, unfortunately for this weathered granite, the clear breaking point (Y point) was not found. Then we selected the most appreciable breaking point and defined it as yield point Y. By this operation, it was found that the strain at Y point was 0.4–1.5% in spite of the different consolidation pressures. Fig. 8 shows that the deviator stress $(\sigma_1-\sigma_3)$ is almost

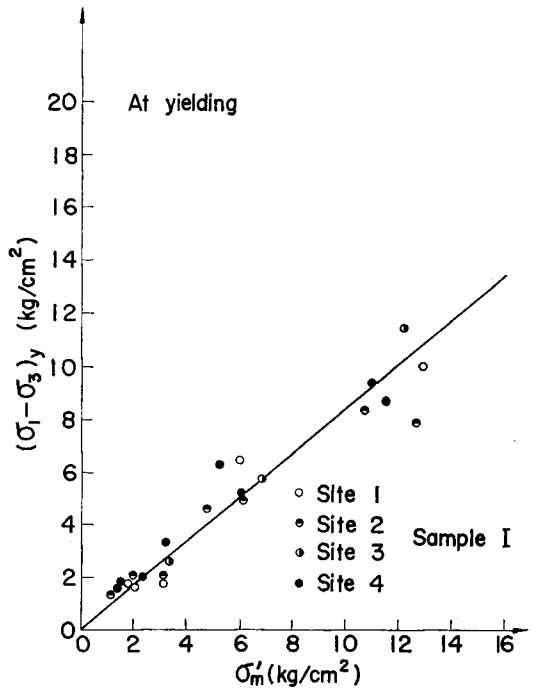

Fig. 8. Strength representation of weathered granite (Sample I) at yielding [point Y] in terms of effective mean stress σ_m'.

linearly dependent upon the mean stress $\sigma_m'=(\tau_1'+2\sigma_3')/3$ at point Y. In order to study the deviation of the data from the straight line, at less than 3 kg/cm^2 of σ_m', Fig. 9 was depicted. $c_{uy}=(\tau_1-\sigma_3)/2$ is the undrained shear stress at point

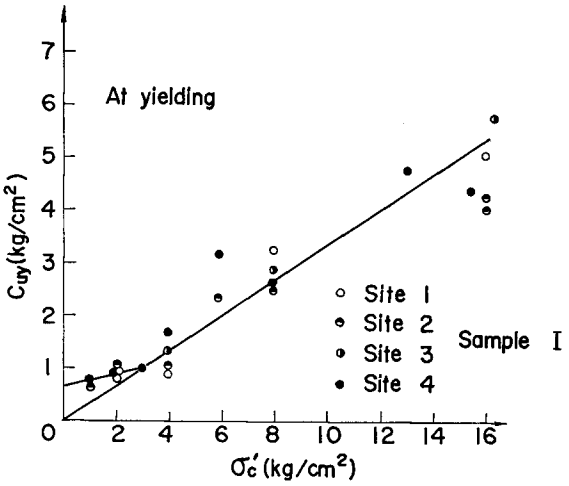

Fig. 9. Strength representation of weathered grainte (Sample I) at yielding [point Y] in terms of consolidation pressure σ_c'.

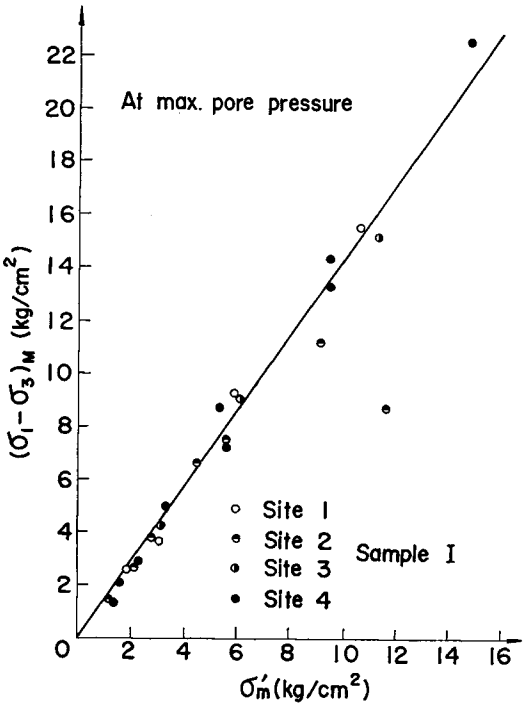

Fig. 10. Strength representation of weathered granite (Sample I) at maximum pore pressure [point M] in terms of effective mean stress σ_m'.

Y and σ_c' is the effective consolidation pressure. From this figure, the over-consolidated region of the sample is clearly seen at $\sigma_m' \leqq 3$ kg/cm^2. The second method is that the turning point of volume change or induced pore pressure (M point as stated above) is determined as a yield point. This M point is close to the point where the effective principal stress ratio σ_1'/σ_3' is maximum.

The strain at point M is greater than at point Y and 1–5.4%. It is less than 2% in the over-consolidated region and more than 3% in the normally consolidated region. Fig. 10 shows that the relation between the deviator stress $(\sigma_1 - \sigma_3)_M$ and the mean effective stress τ_m' is linear, but if Fig. 11 is drawn like Fig. 8, there is a slight deviation from a straight line in the region of the over-consolidation. This "M point" method is very useful in determining the yield point, since the data are directly read from the measuring device, if point Y is unclear. From such determined points Y and M, the parameters of the Mohr-Coulomb type yield criteria are calculated. The cohesion c is nearly 0.0 for both points and the internal friction angle ϕ is 21.6° for Y point and 35.3° for M point, respectively. Fig. 12 shows the yield lines for both Y and M points, and the effective stress paths during the shearing of the specimens. Under the consolidation pressures of 1–2 kg/cm^2, the stress paths rise almost vertically and arrive at the failure line, curving to the right like over-consolidated clay. The stress paths under the consolida-

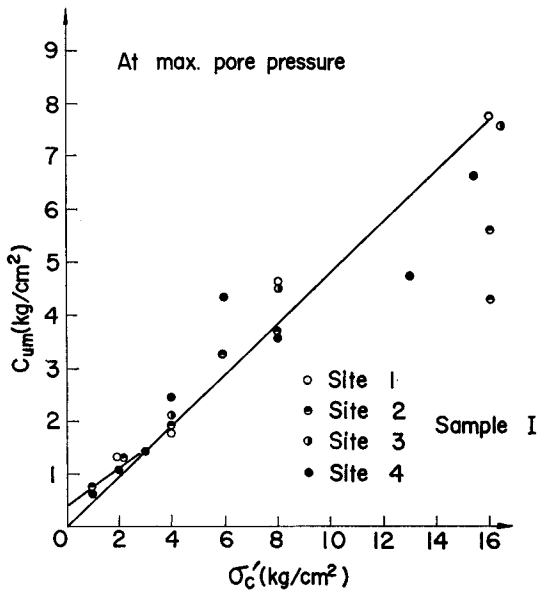

Fig. 11. Strength representation of weathered granite (Sample I) at maximum pore pressure [point M] in terms of consolidation pressure σ_c'.

tion pressures of greater than 3 kg/cm^2 are similar to normally-consolidated clay, and the paths turn to the left with an increase of the induced pore pressure and reach the failure line. However, the paths, after arriving at the failure line, change their direction with a decrease of the pore pressure due to dilatancy, while the strength of the specimen continues to increase.

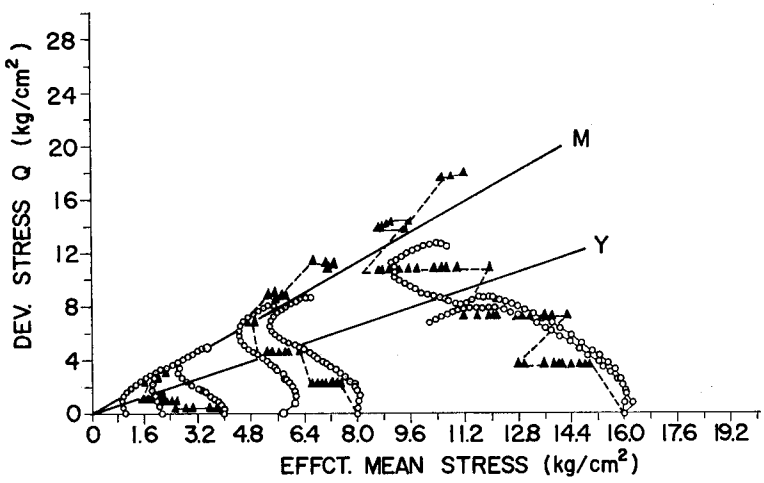

Fig. 12. Stress paths of weathered granite (Sample I).

The ▲ marks in Fig. 12 indicate the stress paths for the triaxial creep test with the same specimens. The creep tests were carried out in order to study the long-term strength of the material. From the figure, the stress paths for the creep tests resemble those of the shear test, although local disagreement seems due to the different loading patterns. It should be noticed that the stress paths of the creep tests also change their tendencies at the line defined from M point by the characteristic change of the induced pore pressure, and the specimens are subjected to failure eventually. The creep strain converges in a short time at a stress level less than the line defined by the Y points. However, at a stress level greater than the Y points, a large creep strain is caused and the specimen goes into a steady state of creep. From these investigations, we can conclude that the Y point defined by the data from the triaxial shear test is the point where the material changes from a stable to unstable state, and the M point is at failure.

(B) Sample II

Sample II is not weathered as much as sample I and is a sandy crystalline material with relatively large grains of quartz, feldspar, *etc.*. This sample is so fragile that it was impossible to take a core by drilling. This difficulty was the most crucial reason why the mechanical properties of this class of rock were not

Table 2. Physical properties of rock sample II
(simbols are same as Table 1)

w	%	6.30
e	—	0.22
γ	g/cm³	2.27
γ_d	g/cm³	2.14
G_s	—	2.61
S_r	%	75.0

known at all.

The way we chose to take a cylindrical sample from a carefully excavated rock block is as follows. The block is confined by wood plates and tapes, and its side was cut one by one. The cut face was immediately covered by a wood plate and tapes. The block is finally cut into an octagonal cylinder shape. It was concluded that this sample shape has no effect on pursuing the triaxial test and the investigation of the mechanical behavior of this rock. This sampling technique is very useful for geologic material whose core is not taken by drilling methods. Table 2 shows the physical properties of this sample II.

(i) Stress-Strain-Pore Pressure

Since the experimental procedure is the same as in the case of sample I, we will not repeat it here. The stress-strain relations are schematically shown in Fig. 13. The stress-strain curves are nearly straight up to 40–50% of the maxi-

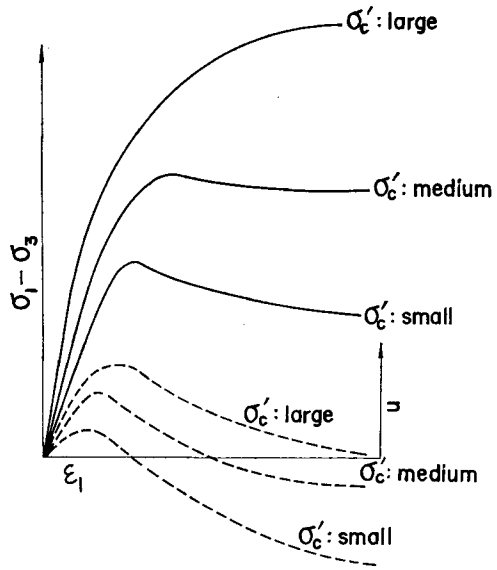

Fig. 13. Behavior of stress-strain-pore pressure of strain-softening type rock subjected to different confining pressures.

mum strength. Afterwards, with a low confining pressure, they have peak stresses and decrease to a residual strength, but with high confinement they don't have a peak and gradually increase. The initial Young's modulus E_i is consolidation pressure dependent as shown in Fig. 14 in a log-log scale, and the relation is obtained in the following equation;

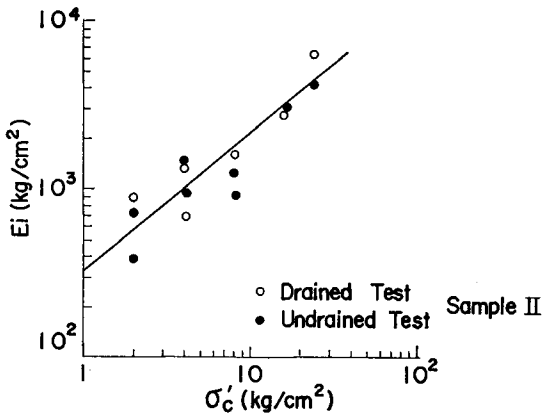

Fig. 14. Variations of initial Young's modulus E_i depending upon the confining pressure σ_c' (Sample II).

$$E_i = 3.25 \times 10^2 \cdot P_a(\sigma_c'/P_a)^{0.82} \qquad (5)$$

It was found that the induced pore pressure during shearing was small due to the unsaturated condition of the sample (degree of saturation 75%) and the magnitude of its peak value is 3–28% of the deviator stress at that point. We tried to saturate the sample in a few days, but did not succeed.

(ii) Strength Parameters

We found that the Y point (a yield point described above) obtained from the tests of sample II was coincident with the point at which the stress-strain curve started deviating from a straight line, and the strain at the point is 0.6–1.9%, independent of the magnitude of the confinement. The strain at M point is calculated as 1–2.7% and the peak stress is reached at 1.5–6.5% of strain with a low confining pressure, depending on the confining.

Fig. 15 shows the effective stress paths of the specimen under various stress conditions. In the figure, it is seen that the stress paths are distinctly different even with the same consolidation pressure. The following reasoning may explain the uncertainty. The different magnitude of the induced pore pressure is mainly due to the difference of the initial degree of saturation, which is heavily influenced by the consolidation pressure, duration time on the saturation before testing, *etc.*.

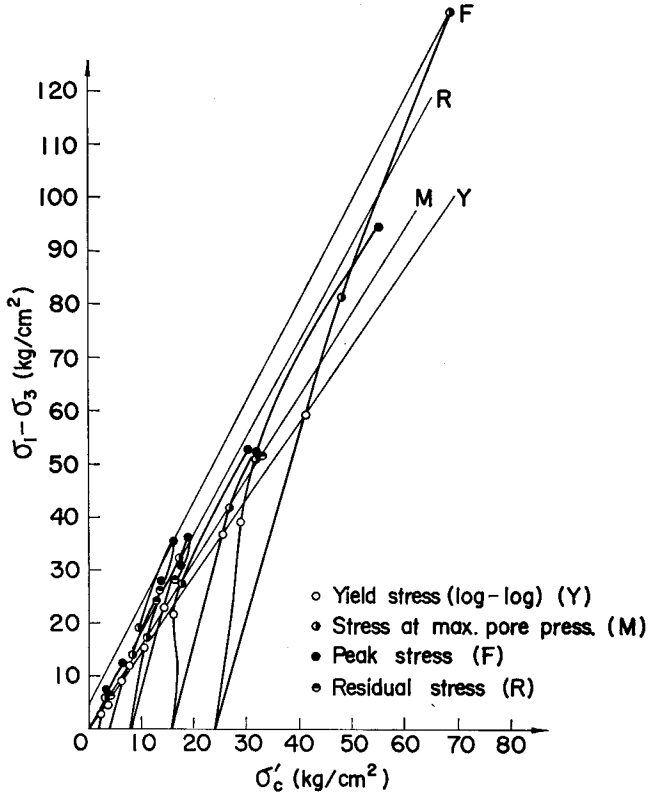

Fig. 15. Stress paths of weathered granite (Sample II).

Table 3. Strength parameters of rock sample II. c': cohesion, ϕ': friction angle (both in terms of effective stress)

	Condition	c'	ϕ'
Y	CU	0 kg/cm^2	34.9°
M	CU	0.60 kg/cm^2	37.7°
F	CU	2.64 kg/cm^2	44.8°
R	CU	0.63 kg/cm^2	43.1°

We have not established the exact way of measuring the degree of saturation simply during shearing. The strength parameters obtained from Fig. 15 are shown in Table 3 for each point of Y, M, F (the peak stress point) and R (the residual strength). It is known that the strength of sample II is greater than that of sample I. The characteristic features of the points Y and M for the failure are the same for both samples I & II. The discussion on the residual strength (R point) was not done due to insufficient data available.

5. Conclusion

Weathered granite whose mechanical properties are not known at all has been tested by the triaxial shearing apparatus in our laboratory, and their strength parameters which are to be applied to the design of the civil engineering structures and foundations were determined. Some of the noticeable experimental results of weathered granite are as follows.

(a) The mechanical behavior of the granite is very similar to that of soil. The methods available in soil mechanics can be used to analyze its behavior.

(b) The failure criterion can be expressed by the Mohr-Coulomb type. Point Y defined in the log-log scale is the failure point for the long-term stability. Point M defined by the point of the peak induced pore pressure is where the material can not sustain the load any more, and such a failure line is used only for a short-term stability analysis.

(c) The initial Young's modulus E_i is highly dependent upon the consolidation pressure.

(d) Sample I shows a strain-hardening type stress-strain curve and sample II shows strain-softening at low confining pressures and strain-hardening with high confinement.

References

1) Kondner, R. L.; "Hyperbolic stress-strain response: Cohesive soil" Journal of the soil mechanics and foundation division, ASCE **89**, No. SM1, Feb. (1963).

2) Duncan, J. M. and C. Y. Chang; "Nonlinear analysis of stress and strain in soils", Journal of the soil mechanics and foundation division, ASCE, **96**, No. SM5, Sept. (1970).